Progress Report

Intraplate Earthquakes in the central-eastern United States: An integrated seismological and geodynamic study

Award #: 04HQGR0046

Principal Investigators: Mian Liu and Eric Sandvol

Dept. of Geological Sciences, University of Missouri
101 Geology Building, UMC, Columbia, MO 65211, USA

Phone: (573) 882-3784; Fax: (573) 882-5458
lium@missouri.edu, http://www.missouri.edu/~geolliu

Key Words: Regional modeling; Seismotectonics; Thermophysical Modeling; Fault dynamics

Non-technical Summary

The project is to use seismology and geodynamic modeling to understand lithospheric structure and stress evolution in the New Madrid Seismic Zone (NMSZ) and other parts of the central-eastern US. So far we have completed 1) a 3D viscoelastic modeling of stress evolution following the 1811-1812 NMSZ large earthquakes; 2) a preliminary integration of seismological studies and dynamic modeling on intraplate earthquakes in the CEUS; 3) a Pn tomography study of the central-eastern US.

A. REPORT OF PROGRESS IN YEAR 2: GEODYNAMIC MODELLING AND SIESMIC IMAGING OF SEISMIC ZONES IN CENTRAL-EASTERN USA

Summary: During the second year of this project we expanded our geodynamic modelling of the New Madrid Seismic Zone (NMSZ) to other parts of CE USA and investigated the fundamental differences between intraplate and interpolate earthquakes in terms of stress evolution in the fault zones. We also produced the preliminary Pn tomography of the lithospheric/upper mantle structure of the region.

Publications:

Li, Q., M. Liu, and A. Sandvol Eric, Stress Evolution Following the 1811-1812 Large Earthquakes in the New Madrid Seismic Zone, Geophys. Res. Lett, 32 (L11310), doi:10.1029/2004GL022133, 2005.

Li, Q., M. Liu, Z. Qie, and A. Sandvol Eric, Stress evolution and seismicity in the central-eastern USA: insights from geodynamic modeling, in Intracontinental earthquakes, edited by S. Stein, and S. Mazzotti, pp. accepted, Geological Society of America, Boulder, Colorado, 2005.

Q. Zhang and A. Sandvol Eric, Pn tomography of central-eastern United States, AGU meeting abstract, 2004.

1. INTRODUCTION

The plate tectonics theory provides a successful geodynamic framework for understanding most earthquakes that occur within the plate boundary zones; however, it offers no ready explanation for earthquakes in the presumably rigid plate interior. One such example is the central-eastern United States (CEUS), defined broadly as the region of continental USA east of the Rocky Mountains. The CEUS is located in the middle of the North America plate where Cenozoic crustal deformation is minimal; however, both historic earthquakes and instrument-recorded earthquakes are abundant (Fig. 1). Major seismic zones in the CEUS include the following (Dewey et al., 1989) (Fig. 1):

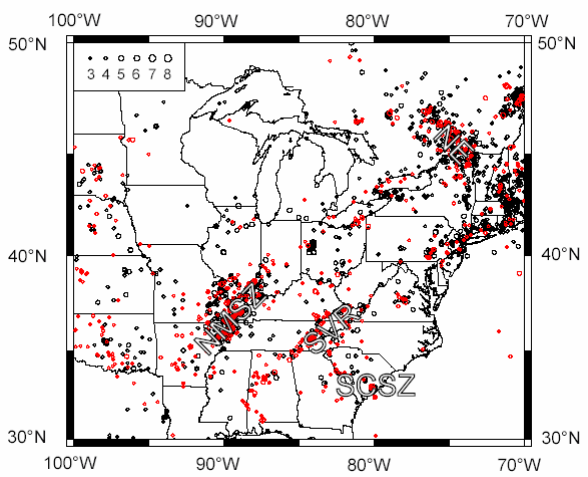

Figure 1. Seismicity in central-eastern United States (CEUS) from NEIC catalog. Black circles: historic events (1800-1973); red circles: modern events (1973-2004). Major seismic zones include the New Madrid seismic zone (NMSZ); the Southern Valley and Ridge (SVR); the South Carolina Seismic Zone (SCSZ); the New England and the St. Lawrence River Valley seismic zone (NE).

1) *The New Madrid seismic zone (NMSZ) and the Mississippi Embayment*: this was the site for the famous 1811-1812 large earthquakes. The magnitudes of the largest three events were Mw 7-7.5 (Hough et al., 2000). Paleoseismological results indicate at least two major earthquakes around 900 and 1400 AD (Kelson et al., 1996; Tuttle et al., 2002). Modern instrumentation has recorded thousands of events since 1977 (Fig. 1).

2) *Southern Valley and Ridge:* also referred to as the eastern Tennessee seismic zone, where modern seismicity is concentrated beneath the Valley and Ridge province, near the western edge of that part of the Appalachians. The largest historical earthquake in this region was the magnitude 5.8 Giles County, Virginia, earthquakes of May 31, 1897 (Nuttli et al., 1979).

3) *South Carolina seismic zone:* The best-known event in this region was the destructive (M~ 6.5-7.0) event that occurred near Charleston, South Carolina, on August 31, 1886 (Nuttli et al., 1979). Paleoseismological studies indicate at least two prehistoric earthquakes in the past 3000 years (Obermeier et al., 1985; Talwani and Cox, 1985).

4) *New England and the St. Lawrence River Valley:* Earthquake epicenters in central New England, upstate New York, and adjacent Canada form a northwest-trending belt of seismicity, sometimes called the Boston-Ottawa zone (Diment et al., 1972; Sbar and Sykes, 1973). The largest historic earthquake in the U.S. part of the Boston-Ottawa zone was probably the Cape Ann, Massachusetts, earthquake of 1755 (M~6, Street and Lacroix, 1979). Further north in the St. Lawrence River valley, numerous events with magnitude 6-7 have been recorded.

Despite intensive studies, the mechanics of earthquakes in the CEUS remain poorly understood. Some workers have suggested that these seismic zones are locales of ancient rifts, thus proposing crustal weakness as the main cause of these earthquakes (Johnston, 1996; Johnston and Kanter, 1990). Others have suggested stress concentration by various factors, including regional and local crustal structures, as the main cause (Grana and Richardson, 1996; Grollimund and Zoback, 2001; Kenner and Segall, 2000; Pollitz et al., 2001a; Stuart et al., 1997). Most workers agree that these intraplate earthquakes are fundamentally different from interplate earthquakes at plate boundaries, yet besides the obvious differences in their strain rates, it remains unclear how intraplate earthquakes fundamentally differ from interplate earthquakes. In this study we first explore the basic mechanical behaviors of intraplate seismic zones and compare them to that of interplate seismic zones. We then apply the results to investigate the seismicity in the NMSZ. In the last part of this paper we present a regional geodynamic model of CEUS, constrained by the lithospheric structure derived from seismic studies by others and our new results of Pn tomography of the CEUS.

2. THE MEHANICS OF INTRAPLATE VS. INTERPLATE SEISMIC ZONES

We have developed three-dimensional viscoelastic models to explore the differences in stress evolution between intraplate and interplate seismic zones. In the models we consider two contrasting properties of these seismic zones: 1) intraplate seismic zones are of finite length, surrounded by strong ambient crust, whereas interplate seismic zones are effectively infinite long (plate boundaries); 2) tectonic loading for intraplate seismic zones are applied at far-field plate boundaries, typically producing low strain rates, whereas interplate seismic zones are loaded directly by relative motions of tectonic plates with relatively high strain rates (Fig. 2). To illustrate the basic physics, we have kept the models relatively simple. The model rheology is linear viscoelastic (Maxwell media). Both models include a 20 km thick stiff upper crust and a ductile lower crust. The viscosity for the upper crust is taken to be 8.0×10^{23} Pa s, making the upper crust essentially elastic for timescales considered here (thousands of years). For the lower crust a range of viscosity values (1.0×10^{19} - 1.0×10^{21} Pa s) is explored for the effects of postseismic relaxation. The model domain is 500 x 500 km. For the intraplate model (Fig. 2a), a 150 km long fault zone is used to simulate a finite seismic zone. The boundary conditions include 0.5 mm/yr compression imposed on the two sides of the model domain. The resulting strain rate is ~2.0×10^{-9}/yr, close to the upper bound for the CEUS (Gan and Prescott, 2001; Newman et al., 1999). The Young's modulus and the Poisson's ratio are taken to be 8.75×10^{10} Pa and 0.25, respectively, for the entire crust (Turcotte and Schubert, 1982). For the interplate model, the fault zone cuts across the entire model domain (Fig. 2b), and the boundary condition is 10 mm/yr on both sides, causing an average slip rate of ~28 mm/yr along the fault zone in the model, similar to that on the San Andreas Fault (Becker et al., 2005; Bennett et al., 2004). In both models the fault zones are represented using special elements that simulate earthquakes with instant plastic strain needed to bring the stress below the yield strength on the fault segments (Li et al., 2005).

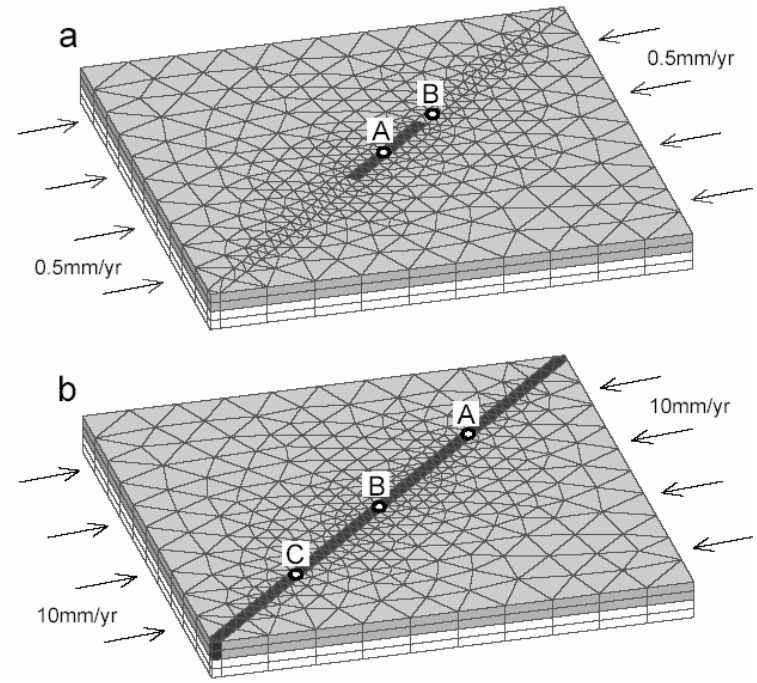

Figure 2. Finite element models for Intraplate (a) and interplate (b) seismic fault zones (in dark). The points are where stress evolution are traced and shown in Figures 4 and 7.

2.1. Intraplate seismic zones

Many seismic zones in the CEUS are marked by some large earthquakes in the past. In this work we chose to avoid speculations of the initial triggering mechanism of these events and instead to focus on stress evolution in the seismic zones following a large earthquake.

Figure 3 shows the calculated evolution of the Coulomb stress following a large intraplate earthquake. The Coulomb stress on a plane is defined as

$$\sigma_f = \tau_\beta - \mu\sigma_\beta \tag{1}$$

where τ_β is the shear stress on the plane, σ_β is the normal stress, and μ is the effective coefficient of friction (King et al., 1994). In regions outside the main fault zone, we calculate the optimal Coulomb stress, which is the stress on planes optimally orientated for failure (King et al., 1994). We assume that initially everywhere in the model upper crust the stress is close to the yield strength, a condition applicable to many continental interiors (Townend and Zoback, 2000; Zoback et al., 2002) and consistent with the widely scattered seismicity in and around the seismic zones in the CEUS (Fig. 1). The model started with a large earthquake, simulated by a 7.5-meter sudden slip across the entire fault plane. This event is equivalent to an M ~ 8.0 earthquake, which caused ~5 MPa stress drop within the fault zone. Coseismic stress release from the fault zone migrates to the tip regions of the fault zone and loads the lower crust below the fault zone. Postseismic viscous relaxation in the lower crust then causes the stress to reaccumulate within the upper crust, mainly near the tips of the fault zone. Similar results have been reported in previous viscoelastic models (Freed and Lin, 2001; Pollitz et al., 2001b). Note

that 200 years after the main earthquake, the fault zone remains in a stress shadow where the stress relieved during the earthquake has not been fully restored. This is mainly because of the slow tectonic loading, whose effects are insignificant over 200 years (compare with Fig. 3b and 3c). The results in Figure 3 were obtained by assuming a complete healing of the fault zone, such that the yield strength returned to the original level immediately following the large event. If the fault zone was unhealed or partially healed, stress reaccumulation within the fault zone would be even slower.

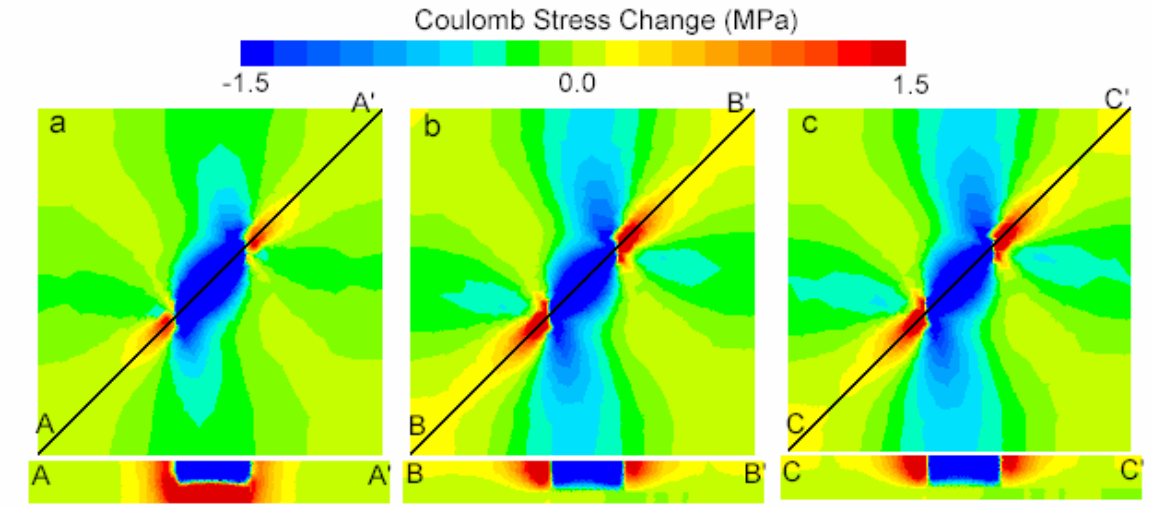

Figure 3. Predicted Coulomb stress change following a large earthquake in an intraplate seismic zone. (a) Co-seismic stress change. (a) The sum of co-seismic and post-seismic (200 years) stress change. (c) Same as (b) but without boundary loading. The bottom panels are depth sections, with 200% vertical exaggeration.

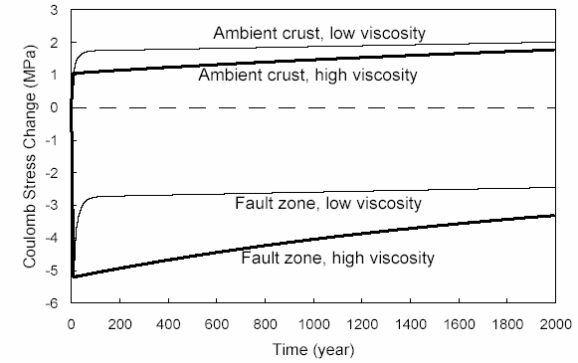

Figure 4. Predicted Coulomb stress evolution in the fault zone (point A in Fig. 2a) and the ambient crust near the fault tips (point B in Fig. 2a) with two values for the lower crust viscosity: high (10^{21} Pa s); low (10^{19} Pa s). The Coulomb stress in the fault zone drops instantly in an earthquake, the initial stress restoration is accelerated by viscous relaxation in the lower crust, and the rate is sensitive to the viscosity. Further stress restoration is mainly controlled by tectonic loading.

In addition to the rate of tectonic loading, postseismic stress evolution depends on the rheology of the lithosphere, especially the lower crust. Fig. 4 shows the effects of lower crustal viscosity on the modeled stress evolution within the fault zone and in the upper crust of the fault tip regions. A lower viscosity of the lower crust will cause more rapid viscous relaxation and stress reloading in the upper crust, but without fast tectonic loading from the far-field, the total amount of stress restoration within the fault zone is largely determined by the stress relieved from the earthquake. For the viscosity range typical of the lower crust (10^{19} – 10^{21} Pas), the results in Fig. 4 show that viscous

relaxation and far-field loading for thousands of years after the major earthquake could not fully restore stress in the fault zone. This may be a fundamental difference between intraplate and interplate seismic zones; the latter is directly loaded by plate motions at high rates, and a ruptured fault segment can also be influenced by earthquakes in the nearby fault segment (see below).

Associated with the stress evolution is a migration and accumulation of strain energy. In the model the strain energy is calculated as

$$E = \frac{1}{2}\sigma'_{ij}\varepsilon'_{ij} \tag{2}$$

where σ'_{ij} and ε'_{ij} are deviatoric stress and strain tensor respectively, using the Einstein summation convention for indexes i and j. Fig. 5 shows the coseismic and postseismic changes of stain energy. Similar to the stress change (Fig. 3), most of the increase of strain energy is near the tips of the fault zone. Because of the slow tectonic loading, much of the strain energy is inherited from the main shock. It would take thousands of years for the far-field tectonic loading to accumulate a comparable amount of strain energy.

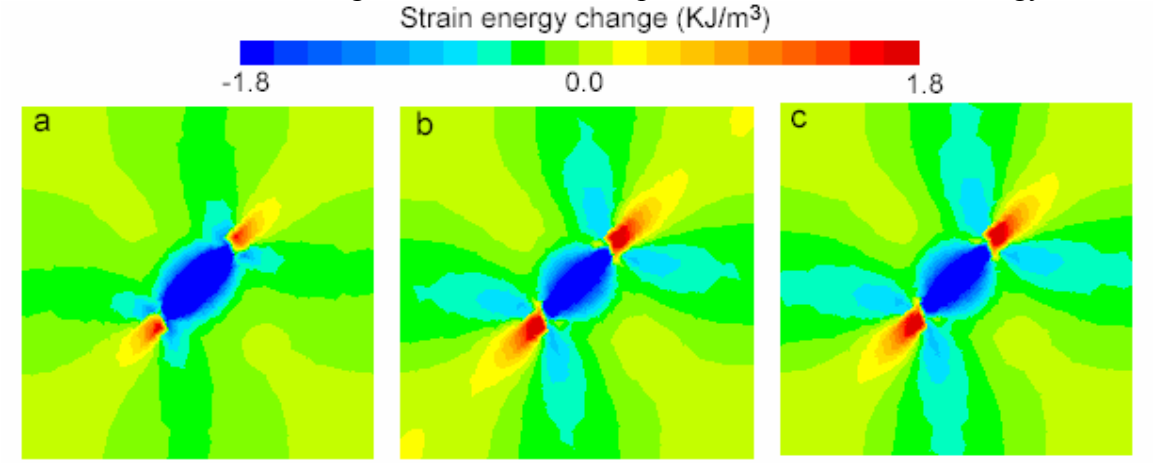

Figure 5. Predicted strain energy change in map view. (a) co-seismic strain energy change. (b) Total strain energy change 200 years after the main shock. (c) Same as (b) but without that tectonic loading. The similarity with (b) shows the dominance of the inherited strain energy over 200 years following the main shock.

2.2 Interplate seismic zones

The stress and strain energy evolution in intraplate seismic zones may be better appreciated when it is contrasted with that of interplate seismic zones (Fig. 2b). Some of the processes are similar. When an interplate earthquake occurs, stress is relieved from the ruptured segment and migrates to the lower crust and to the tip regions of the ruptured segment. Viscous relaxation in the lower crust would then reload the upper crust including the ruptured fault segment, similar to intraplate seismic zones. However, the high strain rates associated with plate motions means that stress can be restored in the ruptured segment more quickly than in intraplate fault zones, and having an infinite long

fault zone (plate boundary) means earthquakes would be largely confined within, and

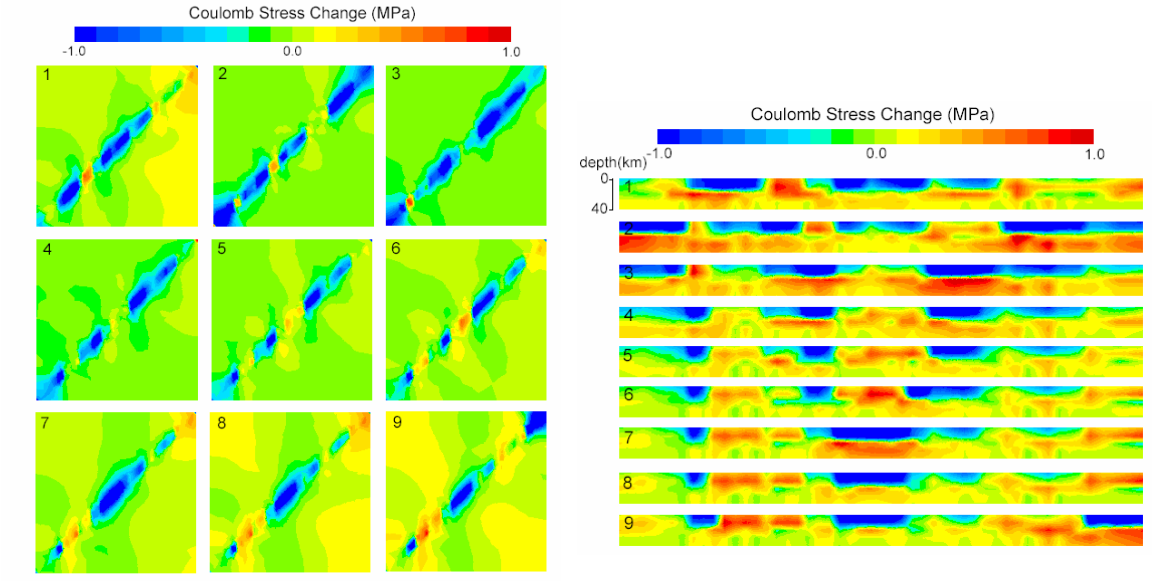

(a) (b)

Figure 6. (a) Snapshots of the predicted stress evolution (map view) for the model of interplate seismic zone (Fig. 2b). The time interval between the panels is 20 years. The sequence shows a selected period of the simulations of stress changes with ruptures of the high stress segments. (b) Depth sections of the predicted stress evolution shown in Fig. 6a. The label of the panels corresponds to the map view panels in Fig. 6a.

migrate along, the fault zone (Fig. 6a). Usually other segments would rupture before earthquake repeats on the same segment (Fig. 6b). Thus for each segment of the ruptured fault zone, postseismic stress recovery may be affected by three major factors: tectonic loading, viscous relaxation, and stress migration caused by nearby earthquakes. This may be better illustrated in Fig. 7, which shows stress evolution at three neighboring points in the fault zone. An earthquake at one of these points causes an instant stress drop. Postseismic stress restoration at the ruptured segment is usually accelerated within the first few tens of years, because of stress migrated from the lower crust by viscous relaxation, in addition to the tectonic loading. Following that is a period of roughly steady-state stress buildup owning to tectonic loading, but a sudden jump of stress may occur when a nearby segment ruptures, which may trigger a new earthquake. Such dynamic behavior has been reported in many interplate seismic zones including the San Andreas Fault (Lin and Stein, 2004; Rydelek and Sacks, 2001; Stein et al., 1997).

One major result for the intraplate seismic zone is that some of the strain energy released from a large earthquake will migrate to the surrounding regions and dominate the local strain energy budget for thousands of years. This is generally not true for interplate seismic zones, where the evolution of strain energy is dominated by tectonic loading. Fig. 8 shows one selected episode of the model experiment. Following an earthquake, the postseismic energy evolution is influenced by strain energy migration from the ruptured segment, viscoelastic reloading, and tectonic loading. Fig. 8c and d compare the strain energy in the model crust 200 years after the earthquake, with and

without tectonic loading. Clearly the effects of tectonic loading are predominant. To show the cumulative strain energy produced from tectonic loading, we artificially prohibited earthquakes for the period shown here. In reality the strain energy evolution will be modulated by frequent ruptures of segments of the interseismic fault zone, as shown in Figs. 6-7.

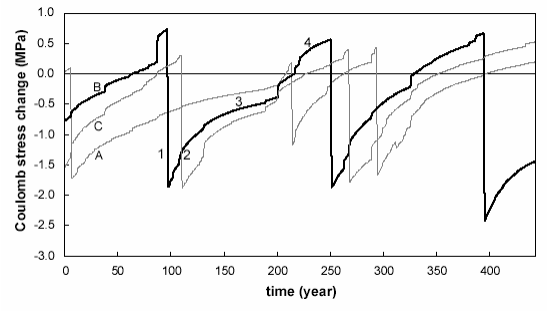

Figure 7. Predicted Coulomb stress evolution at three points on the interplate seismic fault zone (see Fig. 2b). At each point the cycle of stress evolution include four stages: (1) stress drop in an earthquake; (2) accelerated stress restoration because of viscous relaxation of the lower crust; (3) steady stress increase mainly from tectonic loading, and (4) stress jump owning to triggering effect of nearby earthquakes.

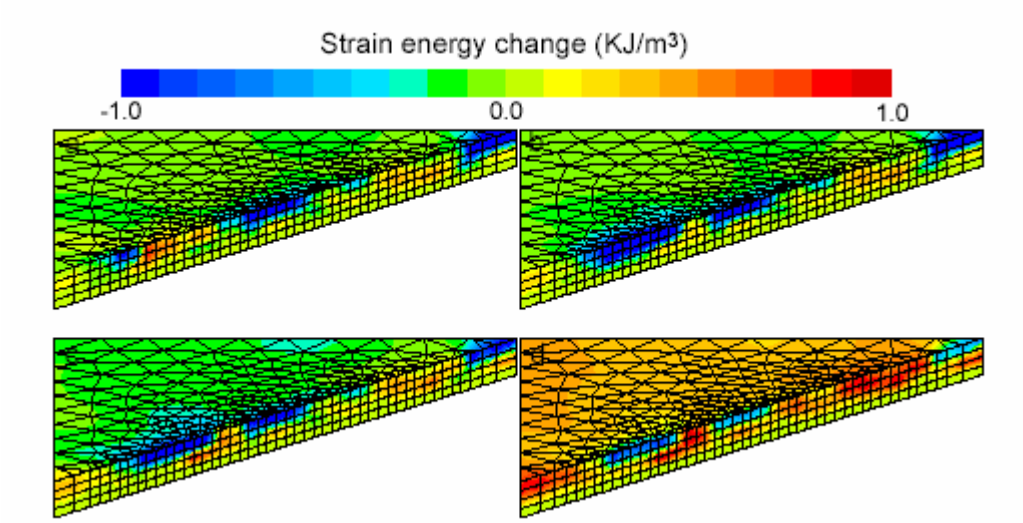

Figure 8. Predicted evolution of strain energy in an interplate seismic zone for a selected period. (a) energy distribution before an earthquake event (the segment with high energy near the left end is the future rupture zone); (b) energy distribution immediately after the earthquake, (c) energy distribution after 200 years without tectonic boundary loading, (d) energy distribution after 200 years with tectonic boundary loading.

3. STRESS EVOLUTION AND SEISMICITY IN THE NMSZ

In this section we apply the model of stress evolution in intraplate seismic zones to the NMSZ, perhaps the best known seismic zones in the CEUS. Within three months in the winter of 1811-1812, at least three large earthquakes occurred here. The magnitudes of these events are estimated to be 7-7.5 (Hough et al., 2000). Since then a dozen or so major events (M 5-6) have occurred in the NMSZ and surrounding regions, and thousands of events have been recorded by modern instruments in the past few decades (Fig. 9).

The NMSZ fault zone is generally delineated by the seismicity. Only one segment of the fault system, the NW trending Reelfoot Fault, is exposed to the surface. Other parts

of the NMSZ fault zone, including the southwestern segments (the Blytheville arch and the Blytheville Fault Zone) and the northeastern segment (the New Madrid North Fault), are inferred mainly by seismicity, reflection and aeromagnetic data (Hildenbrand and Hendricks, 1995; Johnston and Schweig, 1996). The Reelfoot fault is a reverse fault; the southwestern and northeastern segments are inferred to be right-lateral faults from morphologic and geologic features (Gomberg, 1993). These faults are believed to be within a failed rift system formed in Late Proterozoic to Early Cambrian times (Ervin and McGinnis, 1975). We hereinafter use NMSZ when refer to the geographic region of concentrated seismicity, and the NMSZ fault zones when referring to these fault structures.

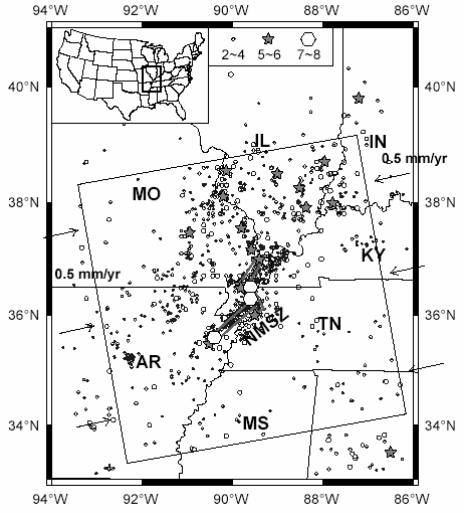

Figure 9. Earthquake epicenters in the NMSZ and surrounding regions (the inset shows the location). Modern earthquake data (for events M>2 since 1974, circles) are from the NEIC and CERI Catalog (1974-2003); pre-1974 and historic earthquake data (M>5, stars) are from Stover and Coffman (1993). Hexagons show the large 1811-1812 events (Stover and Coffman, 1993). The NMSZ is delineated by grey lines. The frame and arrows show the model domain and boundary conditions.

The results in the previous section indicate that following the 1811-1812 large earthquakes, the NMSZ fault zone would still remain in the stress shadow where Coulomb stress is lower than the pre-1811-1812 level, a condition unfavorable for repeating of the large earthquakes. This would have important implications for assessing earthquake hazards in the NMSZ. Here we further explore this issue with a more realistic model (Fig. 9). The NMSZ fault zones are represented in the model by two vertical strike-slip branches connected by the NW-trending reverse fault dipping 45˚ southwest, based on inferred fault geometry (Chiu et al., 1992; Mueller and Pujol, 2001). The compressive stresses across the North American plate were simulated by applying a 0.5 mm/yr velocity boundary condition on the eastern and western edges of the model domain (Fig. 9). This produces a strain rate of ~$2x10^{-9}$/yr within the model domain, which is likely the upper bound of internal deformation rate within the North American plate based on GPS and seismological data (Anderson, 1986; Newman et al., 1999; Zoback et al., 2002). Other model parameters, including the initial conditions and rheological structures, are similar to those in Fig. 2a.

Because our focus is on stress evolution following the large 1811-1812 earthquakes, we simulated these three events as having occurred simultaneously along the entire fault zones. This was simulated with ~5 m instant slip along the model fault zones, resulting in a Coulomb stress drop of 5 MPa within the fault zones, as estimated by Hough et al. (2000). Figure 10 shows the calculated Coulomb stress evolution following the 1811-1812 events. In the upper crust the maximum stress increases are near the NE and SW ends of the NMSZ fault zones. Conversely, stress decreases within the NMSZ fault zones and along a broad zone extending roughly NNW-SSE across the NMSZ. The general pattern is similar to that in Fig. 3.

Each of the large 1811-1812 event was followed by numerous large aftershocks (M>6.0) (Johnston and Schweig, 1996), and since 1812 a dozen or so moderate sized events (M>5) occurred in the NMSZ and surrounding regions (Fig. 9). Although not all these events were included in the calculation, their effects are likely minor in terms of energy release. This can be seen from the stress changes associated with two of the largest earthquakes in the NMSZ region since 1812: the 1895 Charleston, Missouri earthquake (M=6.2) and the 1843 Marked Tree, Arkansas earthquake (M=6.0). The results show some local stress changes near the epicenters of these events, but the general stress pattern remains to be dominated by the 1811-1812 large events. Two hundred years after the 1811-1812 large earthquakes, the NMSZ remains in a stress shadow where stress has not reached the pre-1811-1812 level. The largest Coulomb stress increases are in southern Illinois and eastern Arkansas. Interestingly, these are where most of the major earthquakes (M>5) since 1812 have occurred (Fig. 10).

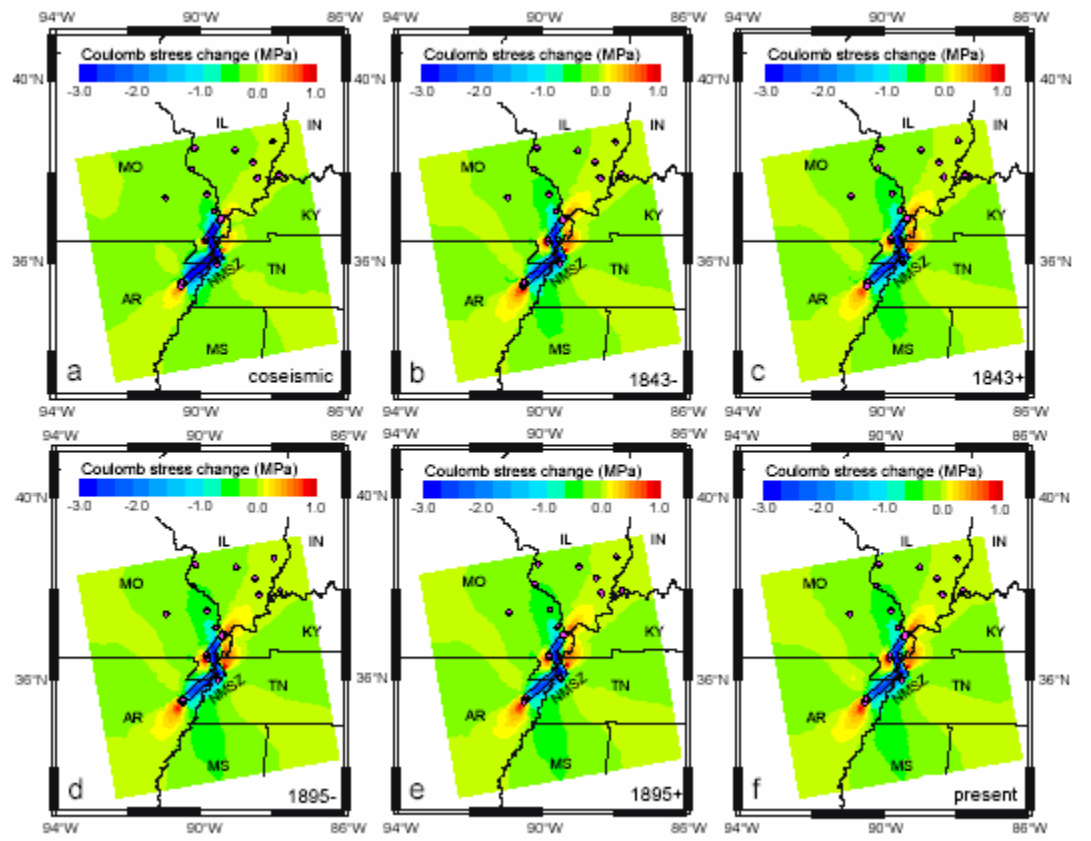

Figure 10. Predicted Coulomb stress evolution in the NMSZ and surrounding regions following the 1811-1812 large events. (a) coseismic; (b) before the 1843 Marked Tree, Arkansas, earthquake; (c) after the 1843 Marked Tree event; (d) before the 1895 Charleston, Missouri, earthquake, (e) after the 1895 Charleston event. (F) at present. The red dots are the epicenters of the major events (M>5) since 1812 (Stover and Coffman, 1993).

The predicted stress evolution is consistent with seismic energy release in the NMSZ and surrounding regions following the 1811 -1812 large events. Figure 11a shows the calculated seismic energy release based on historic and modern earthquake data from

the National Earthquake Information Center (NEIC) catalog (http://neic.usgs.gov/neis/epic/epic.html). We used the Gutenberg-Richter formula (Lay and Wallace, 1995), and approximated all magnitudes as M_S. The spatial pattern is dominated by a dozen moderate sized events (M>5) since 1812, especially the two M~6 events near the NE and SW tips of the NMSZ (Fig. 9). The released seismic energy can be compared with the change of strain energy following the 1811-1812 large earthquakes. Fig. 11b shows the excess strain energy, calculated by assigning a strain change in each element, if needed, to bring the deviatoric stress below the yield strength of the crust during a time step. The total excess strain energy accumulation over a single time step at a given place is given by a vertical integration of the product of stress and the strain change. The spatial pattern of the calculated excess strain energy is consistent with the seismic energy release in the past two centuries (Fig. 11a), but the magnitude is two to three orders higher, presumably because not all energy has been released via earthquakes. The relation between strain energy before the large earthquakes, the energy released during them, and the fraction of energy radiated as seismic waves remains unclear (Kanamori, 1978). It is possible that the portion of the energy release radiated as seismic waves (a fraction called the seismic efficiency) is only ~10% (Lockner and Okubo, 1983). Multiplying the estimated seismic energy release (Fig. 11a) by a factor of 10 provides an estimate of total energy released by earthquakes. Subtracting it from the excess strain energy in Figure 11b gives the residual strain energy, some of which may be released by future earthquakes. The partition between seismic and aseismic energy is uncertain and may range from 2% to 80% (Ward, 1998). Fig. 11c shows the estimated seismic energy in the NMSZ region assuming 10% of the total excess strain energy will be released in future earthquakes. This energy is still capable of producing a number of Mw 6-7 earthquakes in southern Illinois and eastern Arkansas today.

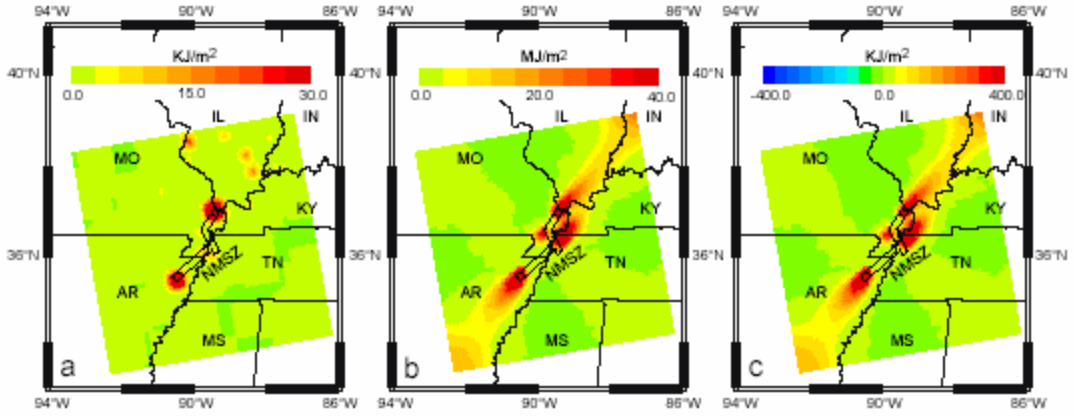

Figure 11. (a) Estimated seismic energy release in the NMSZ and surrounding regions since 1812. (b) Predicted total excess strain energy since the 1811-1812 events. (c) Predicted seismic strain energy in the crust today available for producing earthquakes assuming 10% of the total excess strain energy will be released in future earthquakes.

Thus the basic mechanics illustrated by the simple model of intraplate seismic zones (Fig. 2a) apply to the NMSZ. Without some kind of local loading, the NMSZ fault zone would have remained in a stress shadow today, and the repetition of large earthquakes within the NMSZ fault zones would be unlikely in the next few hundred years. On the other hand, much of the strain energy released by the 1811-1812 events has

migrated to southern Illinois and eastern Arkansas, which may be at least partially responsible for some of the moderate sized earthquakes since 1812. The residual strain energy in these regions, even without additional contribution from local loading, is still capable of producing some damaging earthquakes today.

4. LITHOSPHERIC STRUCTURE AND SEISMICITY IN THE CEUS

So far our discussion of intraplate earthquakes has focused on postseismic evolution after a large earthquake has occurred. Given the low strain rates in the CEUS and most other stable continents, it remains unclear what caused these large earthquakes in the first place. It has been suggested that that most intraplate earthquakes, especially the large events (Mw>6.0), occurred in ancient rift zones (Johnston and Kanter, 1990). This is true for the NMSZ, which is within the Mesozoic Reelfoot rift system (Ervin and McGinnis, 1975), and most hypotheses of local loading mechanisms responsible for the large earthquakes in the NMSZ are based on inferred properties of the rift, including the sinking of an intrusive mafic body in the rift (Grana and Richardson, 1996; Pollitz et al., 2001a), detachment faulting at the base of the rifts (Stuart et al., 1997), and a ductile weak zone under the rift (Kenner and Segall, 2000). However, from Fig. 12, it is clear that not all seismic zones in the CEUS are associated with rifts, and not all rifts are seismically active. One notable example is the Mid-Continent Rift, one of the most prominent rift systems in the CEUS that is essentially aseismic. On the other hand, most of the earthquakes in the CEUS occurred near the margins of the seismologically inferred North American craton, or the "tectosphere" (Jordan, 1979) defined by the abnormally thick lithosphere.

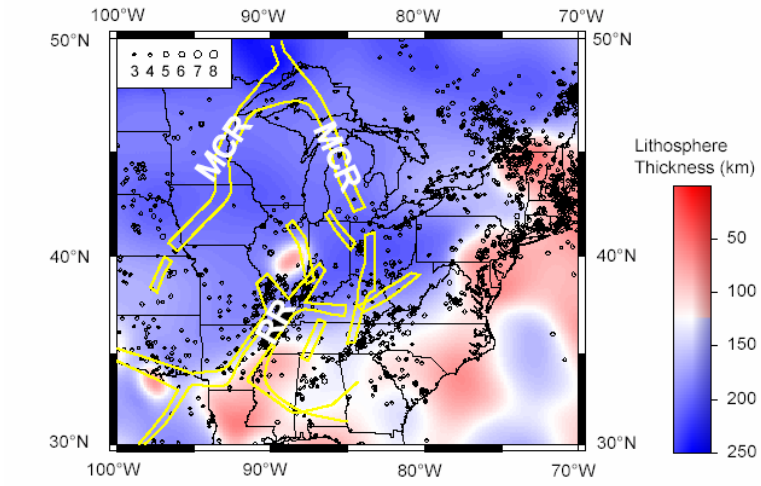

Figure 12. Thermal lithospheric thickness (Goes and van der Lee, 2002) and seismicity (1800-2004) in the CEUS. MCR: Middle Continental Rift; RR: Reelfoot Rift.

4.1 Stress field in the CEUS

Could the lithosphere-tectosphere transition zone concentrate stresses and thus contribute to seismicity in the CEUS? To address this question, we developed a finite element model for the CEUS region (Fig. 13). To simulate the long-term stress pattern, the lithosphere is treated as a power-law fluid continuum with a relative high viscosity

(10^{24} Pa s), underlain by a viscous asthenosphere with a lower viscosity of 10^{21} Pa s. The thickness of the model lithosphere is based on seismologically derived thermal lithosphere thickness (Goes and van der Lee, 2002). The bottom of the model domain is a free slip boundary. The model domain is loaded by a 30 MPa compressive stress at N60ºE on both sides, which is the direction of maximum tectonic compression for the CEUS (Zoback and Zoback, 1989). Fig. 14 shows that calculated Coulomb stress is concentrated in the zones of relatively thin lithosphere, around the margin of the North American tectosphere and under the Mississippi embayment. The regions of high Coulomb stress show a strong spatial correlation with seismic zones in the CEUS, suggesting that the lateral heterogeneity of lithospheric structures is an important factor for seismicity in the CEUS.

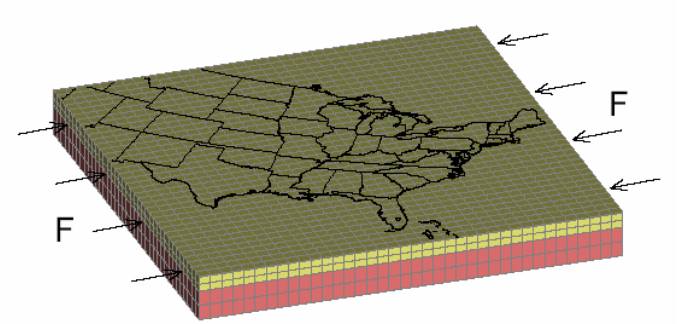

Figure 13. Finite element model for calculating long-term stresses in the CEUS. See text for detail.

4.2 Pn tomography of CEUS

The calculated high Coulomb stress in the Mississippi embayment results from relatively thin lithosphere inferred from low Vs velocities (Goes and van der Lee, 2002) (Fig. 12), which relate to heat flow anomalies in the NMSZ region (Liu and Zoback, 1997). To refine the uppermost mantle velocity structure beneath the central and eastern U.S., we have derived a preliminary Pn velocity map (Fig. 15). Pn is a leaky mode guided wave that travels primarily through the lithospheric mantle and is therefore most sensitive to seismic velocity fluctuations in the uppermost mantle. Pn tomography has become a common method to explore the lithospheric mantle velocity structure (Hearn et al., 1994). This method uses a least squares algorithm (Paige and Saunders, 1982) to iteratively solve for all event-station pairs to obtain slowness, anisotropy, and station and event delays. The method includes damping parameters on both velocity and anisotropy to regularize solution and reduce noise artifacts. P-wave travel time residuals (<10 s) from sources at 1.8^{o} to 15^{o} were used to invert for uppermost mantle velocity. A straight line fit for the initial travel time residuals versus distance gave an apparent Pn velocity of 8 km/s for the study area.

To map the Pn velocity structure in the CEUS, we have collected approximately 11,900 Pn travel times from ISC, NEIC, and from hand picked arrivals taken from both permanent and temporary stations throughout the CEUS. We have hand picked approximately 750 arrivals and combined them with arrivals from the NEIC and ISC. In order to compensate for the relatively small numbers of ray paths, we have used a relatively large cell size in our model parameterization (0.5ºx 0.5º). Overall we have relatively high density of ray paths within the active seismic zones across the CEUS and

relatively low ray coverage in much of the shield portions of the North American plate (Fig. 15a).

We have found a first order agreement between the NA00 model (Goes and van der Lee, 2002) and our Pn tomographic velocity model; however, we have also observed some interesting small scale heterogeneity, such as the surprising low velocities beneath the central Appalachians and Adirondack mountains along the eastern coast of North America (Fig. 15b). The velocities within the Mississippi Embayment and at the eastern margin of the Eastern Tennessee Seismic Zone (ETSZ) are relatively slow (~7.9 km/s). The lithospheric mantle velocities within the North American shield are consistent with the high S-wave velocities measured at 100 km depth. Our results also show relatively low velocities (~7.9 km/s) beneath the Illinois Basin.

The primary difference between our P-wave velocity measurements and the surface wave velocities (Goes and van der Lee, 2002) are within the southern Appalachians. Specifically, near the ETSZ we have found a region of relatively high velocity that is not apparent in the NA00 model. A viscosity contrast and hence a change of lithospheric mantle properties here may help to concentrate stress and thus help explain the ETSZ seismicity.

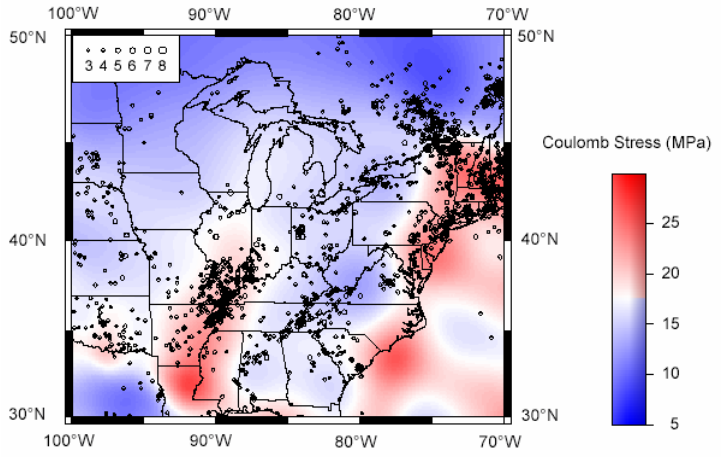

Figure 14. Calculated Coulomb stress. Note the spatial correlation between seismicity and regions of high Coulomb stresses in the CEUS.

5. DISCUSSION

One major result from this study is that the strain energy inherited from large intraplate earthquakes may dominate the local strain energy budget for hundreds to thousands of years after the main shocks. This may be expected, given the generally low strain rates in stable continent including the North American plate interior (Dixon et al., 1996; Gan and Prescott, 2001). Applied to the NMSZ, we have shown that the predicted spatial pattern and values of the stress and strain energy buildup following the 1811-1812 large events may explain the occurrence of many moderate sized earthquakes in areas surrounding the NMSZ since 1812. Furthermore, we have shown that intraplate seismic zones tends to stay in a stress shadow where full stress restoration after large events may take thousands of years, longer than predictions based solely on regional strain rates estimate. This is because seismic zones within a stable continent are of finite length, surrounded by relatively strong crust. As long as deviatoric stresses can be supported by the ambient crust, little stress is available to reload the fault zones. This result is

consistent with recent geodetic measurements in the NMSZ and surrounding regions that show the current strain rates are very slow (0 ± 2 mm/yr) (Gan and Prescott, 2001; Newman et al., 1999), rather than 5-8 mm/yr reported earlier (Liu et al., 1992). These results do not contradict seismicity in the NMSZ. Although thousands of events have been recorded in the NMSZ in the past decades, most of those are micro events (M<4) so the energy release is insignificant. No major (M>5) events have occurred within the NMSZ fault zone since 1812, and the two largest events in the past two centuries, the 1895 Charleston, Missouri earthquake (M=6.2) and the 1843 Marked Tree, Arkansas earthquake (M=6.0), occurred near the tip of the inferred NMSZ fault zones, consistent with the model results.

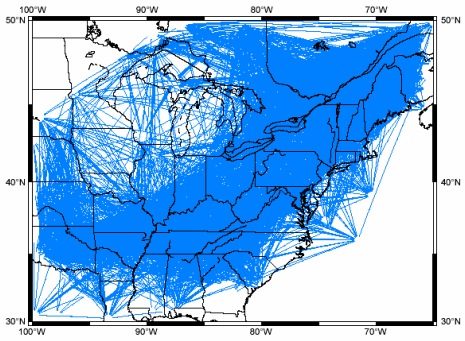

Figure 15. (a) Ray coverage for Pn paths between 2 and 15 degrees distance in the CEUS. Approximately 8900 ray paths are shown in the map. (b) Preliminary Pn tomographic map for the CEUS. Black circles are the same earthquake epicenters shown in Figure 9.

However, the model results are inconsistent with paleoseismological data that indicate at least two more events similar to the 1811-1812 large events occurred in the NMSZ around AD 900 and 1400 (Kelson et al., 1996; Tuttle et al., 2002). Given the difficulties in determining the size and location of paleoearthquakes from liquefaction data, it is no surprising that questions have been raised regarding conclusions drawn from such data. Newman and Stein (1999), for instance, argued that the size of these paleoevents may be overestimated – these may be M~7, rather than M~8, events, more in line with the new estimates for the 1811-1812 events (Hough et al., 2000). However, even for M~7 events to repeat in the NMSZ fault zone every few hundred years is inconsistent with the model predictions. Thus the paleoseismological data require a local loading mechanism. Various local loadings have been proposed, including sinking of a "mafic pillow" within the Reelfoot rift (Grana and Richardson, 1996; Pollitz et al., 2001a) and a weak lower crustal zone under the NMSZ (Kenner and Segall, 2000). We have avoided including these models in our calculations because of the large uncertainties associated with each of them. Because seismic activity in the NMSZ likely started in the Holocene (Pratt, 1994; Schweig and Ellis, 1994; Van Arsdale, 2000), any mechanism of local loading must also explain why it started in the Holocene. Stress triggering associated with glacial isostatic adjustment (GIA) provides some interesting possible causes; James and Bent (1994) and Wu and Johnston (2000) find that GIA may be significant for seismicity in the St. Lawrence valley but not the more distant NMSZ, whereas Grollimund and Zoback (2001) suggest that GIA could be the cause of New Madrid seismicity. Refined imaging of crustal and lithospheric structures under the NMSZ and other seismic zones in the CEUS would help to test potential local loading mechanisms.

The stress field in the CEUS is characterized by a nearly horizontal, NE to E-striking axis of maximum compressive stress (Herrmann, 1979; Sbar and Sykes, 1973;

Zoback and Zoback, 1989). The uniformity of stress-tensor orientation over a broad area of the CEUS suggests that the stress field arises from forces that drive or resist plate motions (Richardson and Solomon, 1979; Zoback and Zoback, 1989). Given the rather uniform far-field stresses and the stability of stable plate interior, crustal weakness, often found in ancient rift zones, is commonly related to intraplate earthquakes (Johnston and Kanter, 1990; Johnston and Schweig, 1996). This seems true in the central US, especially in the Mississippi embayment (Fig. 12), but not in the eastern US, where seismic zones seem spatially associated with ancient faults developed when the eastern United States was near the plate boundaries (Dewey et al., 1989), or faults that may be related to transform fracture zones in the Atlantic ocean floor (Sykes, 1978). Whereas these seismic zones may be associated with different structural causes, we suggest that there may be a common and deep cause for most of the seismicity in the CEUS: the transition zone between the thick North American tectosphere and the surrounding lithosphere. Our calculations show that such lateral heterogeneity of lithospheric structure could cause stress concentration near the margins of the tectosphere, and the predicted regions of high stresses has a strong spatial correlation with seismicity in the CEUS. Further testing of the causative relationship between lithospheric structures and seismicity has to wait for more detailed crustal and lithospheric structures of the CEUS to become available.

6. CONCLUSIONS

Major conclusions we may draw from this study include:

1) Intraplate seismic zones tend to remain in a Coulomb stress shadow for thousands of years following large earthquakes. The slow far-field tectonic loading rates and the relatively strong ambient crust make stress re-accumulation within intraplate fault zones difficult, unless there is some kind of local loading mechanism. On the other hand, a significant amount of the stress relieved from large intraplate earthquakes, and the associated strain energy, may migrate to and be trapped within the ambient crust, mainly near the tip regions of the fault zones. Such inherited strain energy may dominate the strain energy budget in the intraplate fault zone and surrounding regions for hundreds to thousands of years, capable of producing aftershocks hundreds of years after the main shocks. These are some of the fundamental differences from interplate seismic zones, which are constantly loaded by plate motions.

2) The 1811-1812 large earthquakes in the NMSZ caused significant buildup of Coulomb stress and strain energy in the surrounding regions, mainly southern Illinois and eastern Arkansas. Many of the moderate sized earthquakes (M>5) in these regions since 1812 may have been triggered or produced by such stress and strain energy. The residual strain energy from the 1811-1812 main shocks is still capable of producing some damaging (M>6) earthquakes in areas surrounding the NMSZ today, even at the absence of local loading. Conversely, the NMSZ fault zones have remained in a stress shadow where thousands of years may be needed for the stress to restore to the pre-1811-1812 level. Thus, some kind of local loading mechanism would be needed if numerous large events similar to the 1811-1812 events have occurred in the fault zones during the Holocene, as suggested by paleoseismological data. Whereas a number of local loading

mechanisms have been proposed, more studies, including refined imaging of the crustal and lithospheric structures in the NMSZ region, would be needed to test these hypotheses.

3) Seismicity in the CEUS is spatially correlated with the margins of the seismologically inferred North American tectosphere, and our modeling results show that the Coulomb stress tends to concentrate in the tectosphere-lithosphere transition zones. Even in the NMSZ, the seismicity seems to be related to an abnormally thin lithosphere under the Mississippi embayment, in addition to the rift-weakened crust. Again, refined imaging of the crustal and lithospheric structure in the future will help to address the cause of seismicity in the NMSZ and other seismic zones in the CEUS.

Acknowledgements. We have benefited from helpful discussion with Seth Stein, Jian Lin, and Andy Newman. This work is supported by USGS NEHRP grant 04HQGR0046.

References

Anderson, J.G., 1986, Seismic strain rates in the central and eastern United States: Seismological Society of America Bulletin, v. 76, p. 273-290.

Becker, T.W., Hardebeck, J.L., and Anderson, G., 2005, Constraints on fault slip rates of the southern California plate boundary from GPS velocity and stress inversions: Geophysical Journal International, v. 160, p. 634-650.

Bennett, R.A., Friedrich, A.M., and Furlong, K.P., 2004, Codependent histories of the San Andreas and San Jacinto fault zones from inversion of fault displacement rates: Geology, v. 32, p. 961-964.

Chiu, J.M., Johnston, A.C., and Yang, Y.T., 1992, Imaging the active faults of the central New Madrid seismic zone using PANDA array data: Seismological Research Letters, v. 63, p. 375-393.

Dewey, J.W., Hill, D.P., Ellsworth, W.L., and Engdahl, E.R., 1989, Earthquakes, faults, and the seismotectonic framework of the contiguous United States, *in* Pakiser, L.C., and Mooney, W.D., eds., Geophysics Framework of the Continental United States, Volume 172: Boulder, CO, GSA, p. 541-576.

Diment, W.H., Urban, T.C., and Revetta, F.A., 1972, Some geophysical anomalies in the eastern United States, The Nature of the Solid Earth.

Dixon, T.H., Mao, A., and Stein, S., 1996, How rigid is the stable interior of the North American plate?: Geophysical Research Letters, v. 23, p. 3035-3038.

Ervin, C.P., and McGinnis, L.D., 1975, Reelfoot Rift; reactivated precursor to the Mississippi Embayment: Geological Society of America Bulletin, v. 86, p. 1287-1295.

Freed, A.M., and Lin, J., 2001, Delayed triggering of the 1999 Hector Mine earthquake by viscoelastic stress transfer: Nature (London), v. 411, p. 180-183.

Gan, W., and Prescott, W.H., 2001, Crustal deformation rates in central and eastern U.S. inferred from GPS: Geophysical Research Letters, v. 28, p. 3733-3736.

Goes, S., and van der Lee, S., 2002, Thermal structure of the North American uppermost mantle inferred from seismic tomography: Journal of Geophysical Research, v. 107, p. 2050, doi:10.1029/2000JB000049.

Gomberg, J.S., 1993, Tectonic deformation in the New Madrid seismic zone; inferences from map view and cross-sectional boundary element models: Journal of Geophysical Research, B, Solid Earth and Planets, v. 98, p. 6639-6664.
Grana, J.P., and Richardson, R.M., 1996, Tectonic stress within the New Madrid seismic zone: Journal of Geophysical Research, v. 101, p. 5445-5458.
Grollimund, B., and Zoback, M.D., 2001, Did deglaciation trigger intraplate seismicity in the New Madrid seismic zone?: Geology (Boulder), v. 29, p. 175-178.
Hearn, T.M., Rosca, A.C., and Fehler, M.C., 1994, Pn tomography beneath the southern Great Basin: Geophysical Research Letters, v. 21, p. 2187-2190.
Herrmann, R.B., 1979, Surface wave focal mechanisms for eastern North American earthquakes with tectonic implications: Journal of Geophysical Research, v. 84, p. 3543-3552.
Hildenbrand, T.G., and Hendricks, J.D., 1995, Geophysical setting of the Reelfoot Rift and relations between rift structures and the New Madrid seismic zone: U.S. Geological Survey Professional Paper, p. E1-E30.
Hough, S.E., Armbruster, J.G., Seeber, L., and Hough, J.F., 2000, On the modified Mercalli intensities and magnitudes of the 1811-1812 New Madrid earthquakes: Journal of Geophysical Research, B, Solid Earth and Planets, v. 105, p. 23,839-23,864.
James, T.S., and Bent, A.L., 1994, A comparison of eastern North American seismic strain-rates to glacial rebound strain-rates: Geophysical Research Letters, v. 21, p. 2127-2130.
Johnston, A.C., 1996, Seismic moment assessment of earthquakes in stable continental regions; III, New Madrid 1811-1812, Charleston 1886 and Lisbon 1755: Geophysical Journal International, v. 126, p. 314-344.
Johnston, A.C., and Kanter, L.R., 1990, Earthquakes in stable continental crust: Scientific American, v. 262(3), p. 68-75.
Johnston, A.C., and Schweig, E.S., 1996, The enigma of the New Madrid earthquakes of 1811-1812: Annual Review of Earth and Planetary Sciences.
Jordan, T.H., 1979, Mineralogies, densities and seismic velocities of garnet lherzolites and their geophysical implications, The mantle sample; inclusions in kimberlites and other volcanics; Proceedings of the Second international kimberlite conference; Volume 2, Am. Geophys. Union.
Kanamori, H., 1978, Quantification of earthquakes: Nature, v. 271, p. 411-414.
Kelson, K.I., Simpson, G.D., VanArsdale, R.B., Haraden, C.C., and Lettis, W.R., 1996, Multiple late Holocene earthquakes along the Reelfoot Fault, central New Madrid seismic zone: Journal of Geophysical Research, v. 101, p. 6151-6170.
Kenner, S.J., and Segall, P., 2000, A mechanical model for intraplate earthquakes; application to the New Madrid seismic zone: Science, v. 289, p. 2329-2332.
King, G.C.P., Stein, R.S., and Lin, J., 1994, Static stress changes and the triggering of earthquakes: Bulletin of the Seismological Society of America, v. 84, p. 935-953.
Lay, T., and Wallace, T.C., 1995, Modern Global Seismology: San Diego, Academic Press, 383-385 p.
Li, Q., Liu, M., and Sandvol, E., 2005, Stress evolution following the 1811-1812 large earthquakes in the New Madrid seismic zone: Geophysical Research Letters (in review).

Lin, J., and Stein, R.S., 2004, Stress triggering in thrust and subduction earthquakes, and stress interaction between the southern San Andreas and nearby thrust and strike-slip faults: Journal of Geophysical Research, v. 109, p. doi:10. 1029/2003JB002607.

Liu, L., and Zoback, M.D., 1997, Lithospheric strength and intraplate seismicity in the New Madrid seismic zone: Tectonics, v. 16, p. 585-595.

Liu, L., Zoback, M.D., and Segall, P., 1992, Rapid intraplate strain accumulation in the New Madrid seismic zone: Science, v. 257, p. 1666-1669.

Lockner, D.A., and Okubo, P.G., 1983, Measurements of frictional heating in granite: Journal of Geophysical Research, v. 88, p. 4313-4320.

Mueller, K., and Pujol, J., 2001, Three-Dimensional Geometry of the Reelfoot Blind Thrust: Implications for Moment Release and Earthquake Magnitude in the New Madrid Seismic Zone: Bulletin of the Seismological Society of America, v. 91, p. 1563-1573.

Newman, A., Stein, S., Weber, J., Engeln, J., Mao, A., and Dixon, T., 1999, Slow deformation and lower seismic hazard at the New Madrid Seismic Zone: Science, v. 284, p. 619-621.

Nuttli, O.W., Bollinger, G.A., and Griffiths, D.W., 1979, On the relation between modified Mercalli intensity and body-wave magnitude: Bulletin of the Seismological Society of America, v. 69, p. 893-909.

Obermeier, S.F., Gohn, G.S., Weems, R.E., Gelinas, R.L., and Rubin, M., 1985, Geologic evidence for recurrent moderate to large earthquakes near Charleston, South Carolina: Science, v. 227, p. 408-411.

Paige, C.C., and Saunders, M.A., 1982, LSQR: an algorithm for sparse linear equations and sparse least squares: ACM Transactions on Mathematical Software (TOMS), v. 8, p. 43-71.

Pollitz, F.F., Kellogg, L., and Buergmann, R., 2001a, Sinking mafic body in a reactivated lower crust; a mechanism for stress concentration at the New Madrid seismic zone: Bulletin of the Seismological Society of America, v. 91, p. 1882-1897.

Pollitz, F.F., Wicks, C., and Thatcher, W., 2001b, Mantle flow beneath a continental strike-slip fault; postseismic deformation after the 1999 Hector Mine earthquake: Science, v. 293, p. 1814-1818.

Pratt, T.L., 1994, How old is the New Madrid seismic zone?: Seismological Research Letters, v. 65, p. 172-179.

Richardson, R.M., and Solomon, S.C., 1979, Tectonic stress in the plates: Reviews of Geophysics and Space Physics, v. 17, p. 981-1019.

Rydelek, P.A., and Sacks, I.S., 2001, Migration of large earthquakes along the San Jacinto Fault; stress diffusion from 1857 Fort Tejon earthquake: Geophysical Research Letters, v. 28, p. 3079-3082.

Sbar, M.L., and Sykes, L.R., 1973, Contemporary Compressive Stress and Seismicity in Eastern North America; An Example of Intra-plate Tectonics: Geological Society of America Bulletin, v. 84, p. 1861-1881.

Schweig, E.S., and Ellis, M.A., 1994, Reconciling short recurrence intervals with minor deformation in the New Madrid seismic zone: Science, v. 264, p. 1308-1311.

Stein, R.S., Barka, A.A., and Dieterich, J.H., 1997, Progressive failure on the North Anatolian fault since 1939 by earthquake stress triggering: Geophysical Journal International, v. 128, p. 594-604.
Stover, C.W., and Coffman, J.L., 1993, Seismicity of the United States, 1568-1989 (revised): U.S. Geological Survey Professional Paper, p. 418.
Street, R., and Lacroix, A., 1979, An empirical study of New England seismicity: 1727-1977: Bulletin of the Seismological Society of America, v. 69, p. 159-175.
Stuart, W.D., Hildenbrand, T.G., and Simpson, R.W., 1997, Stressing of the New Madrid seismic zone by a lower crust detachment fault: Journal of Geophysical Research, v. 102, p. 27,623-27,633.
Sykes, L.R., 1978, Intraplate seismicity, reactivation of preexisting zones of weakness, alkaline magmatism, and other tectonism postdating continental fragmentation: Reviews of Geophysics and Space Physics, v. 16, p. 621-688.
Talwani, P., and Cox, J., 1985, Paleoseismic evidence for recurrence of earthquakes near Charleston, South Carolina: Science, v. 229, p. 379-381.
Townend, J., and Zoback, M.D., 2000, How faulting keeps the crust strong: Geology, v. 28, p. 399-402.
Turcotte, D.L., and Schubert, G., 1982, Geodynamics: Applications of continuum physics to geological problems: New York, John Wiley & Sons, 450 p.
Tuttle, M.P., Schweig, E.S., Sims, J.D., Lafferty, R.H., Wolf, L.W., and Haynes, M.L., 2002, The earthquake potential of the New Madrid seismic zone: Bulletin of the Seismological Society of America, v. 92, p. 2080-2089.
Van Arsdale, R., 2000, Displacement history and slip rate on the Reelfoot Fault of the New Madrid seismic zone: Engineering Geology, v. 55, p. 219-226.
Ward, S.N., 1998, On the consistency of earthquake moment rates, geological fault data, and space geodetic strain; the United States: Geophysical Journal International, v. 134, p. 172-186.
Wu, P., and Johnston, P., 2000, Can deglaciation trigger earthquakes in N. America?: Geophysical Research Letters, v. 27, p. 1323-1326.
Zoback, M.D., Townend, J., and Grollimund, B., 2002, Steady-state failure equilibrium and deformation of intraplate lithosphere: International Geology Review, v. 44, p. 383-401.
Zoback, M.L., and Zoback, M.D., 1989, Tectonic stress field of the continental United States, *in* Pakiser, L.C., and Mooney, W.D., eds., Geophysical framework of the continental United States, Volume 172: Boulder, CO, United States, Geological Society of America (GSA), p. 523-539.